Inorg. Chem. **2009**, *48*, 3057−3064

Synthesis and Modification of a Functionalized 3D Open-Framework Structure with MIL-53 Topology

Tim Ahnfeldt,[†] Daniel Gunzelmann,[‡] Thierry Loiseau,[§] Dunja Hirsemann,[‡] Jürgen Senker,[‡] Gerard Férey,[§] and Norbert Stock*[,†]

Institute of Inorganic Chemistry, Christian-Albrechts-Universität, Otto-Hahn-Platz 6/7, 24118 Kiel, Germany, Institute of Inorganic Chemistry, University of Bayreuth, Universitätsstrasse 30, 95447 Bayreuth, Germany, and Institut Lavoisier, UMR CNRS 8180, Université de Versailles St-Quentin en Yvelines, 45 Avenue des Etats-Unis, 78035 Versailles, France

Received December 4, 2008

Aluminum aminoterephthalate Al(OH)[H_2N−BDC]·0.3(H_2N−H_2BDC (denoted MIL-53−NH_2(as)) was synthesized under hydrothermal conditions. The activation of the compound can be achieved in two steps. The treatment with DMF at 150 °C leads to Al(OH)[H_2N−BDC]·0.95DMF (MIL-53−NH_2(DMF)). In the second step, DMF is thermally removed at 130 °C. Upon cooling in air, the hydrated form Al(OH)[H_2N−BDC]·0.9H_2O (MIL-53−NH_2(lt)) is obtained. The dehydration leads to a porous compound that exhibits hysteresis behavior in the N_2 sorption experiments. The MIL-53−NH_2(lt) can be modified by postsynthetic functionalization using formic acid, and the corresponding amide Al(OH)[HC(O)N(H)−BDC]·H_2O (MIL-53−NHCHO) is formed. All four phases were thoroughly characterized by X-ray powder diffraction, solid-state NMR and IR spectroscopy, and sorption measurements, as well as thermogravimetric and elemental analysis. Based on the refined lattice parameter similar breathing behavior of the framework as found in the unfunctionalized MIL-53 can be deduced. Solid-state NMR spectra unequivocally demonstrate the presence of the guest species, as well as the successful postsynthetic functionalization.

Introduction

Inorganic−organic hybrids have developed into an important class in the family of porous materials.[1−3] This is due to their interesting magnetic[4,5] or optical properties,[6,7] their potential application in the fields of gas and liquid separation[8,9] and storage,[10,11] their catalysis,[12,13] as well as their drug delivery.[14] The success of hybrid frameworks is based on the diversity of metal oxide clusters that can be connected with innumerous functionalized organic linkers. In the field of metal carboxylates, the use of linear organic linkers, especially terephthalic acid (BDC), is very popular since it gives rise to the formation of many open-framework structures with interesting features.[15] The combination of trivalent metal cations, such as Al^{3+}, V^{3+}, Cr^{3+}, Fe^{3+}, Ga^{3+}, and In^{3+}, and terephthalic acid under solvothermal synthetic conditions results in the formation of at least five crystalline

* To whom correspondence should be addressed. E-mail: stock@ac.uni-kiel.de.
[†] Christian-Albrechts-Universität.
[‡] University of Bayreuth.
[§] Université de Versailles St-Quentin en Yvelines.

(1) Kitagawa, S.; Uemara, K. *Chem. Soc. Rev.* **2005**, *34*, 109.
(2) Rowsell, J. L. C.; Yaghi, O. M. *Microporous Mesoporous Mater.* **2004**, *73*, 15.
(3) Cheetham, A. K.; Rao, C. N. R.; Feller, R. K. *Chem. Commun.* **2006**, 4780.
(4) Maspoch, D.; Ruiz-Molina, D.; Wurst, K.; Domingo, N.; Cavallini, M.; Biscarini, F.; Tejada, J.; Rovira, C.; Veciana, J. *Nat. Mater.* **2003**, *2*, 190.
(5) Halder, G. J.; Kepert, C. J.; Moubaraki, B.; Murray, K. S.; Cashion, J. D. *Science* **2002**, *298*, 1762.
(6) Holman, K. T.; Pivovar, A. M.; Swift, J. A.; Ward, M. D. *Acc. Chem. Res.* **2001**, *34*, 107.
(7) Evans, O. R.; Lin, W. B. *Acc. Chem. Res.* **2002**, *35*, 511.
(8) Alaerts, L.; Maes, M.; Giebeler, L.; Jacobs, P. A.; Martens, J. A.; Denayer, J. F. M.; Kirschhock, C. E. A.; De Vos, D. E. *J. Am. Chem. Soc.* **2008**, *130*, 14170.
(9) Chen, B.; Liang, C.; Yang, J.; Contreras, D. S.; Clancy, Y. L.; Lobkovsky, E. B.; Yaghi, O. M.; Dai, S. *Angew. Chem., Int. Ed.* **2006**, *45*, 1390.
(10) Férey, G.; Latroche, M.; Serre, C.; Millange, F.; Loiseau, T.; Percheron-Guégan, A. *Chem. Commun.* **2003**, 2976.
(11) Rowsell, J. L. C.; Millward, A. R.; Park, K. S.; Yaghi, O. M. *J. Am. Chem. Soc.* **2004**, *126*, 5666.
(12) Fujita, M.; Kwon, Y. J.; Washizu, S.; Ogura, K. *J. Am. Chem. Soc.* **1994**, *116*, 1151.
(13) Evans, O. R.; Ngo, H. L.; Lin, W. *J. Am. Chem. Soc.* **2001**, *123*, 10395.
(14) Horcajada, P.; Serre, C.; Vallet-Regí, M.; Sebban, M.; Taulelle, F.; Férey, G. *Angew. Chem., Int. Ed.* **2006**, *45*, 5974.
(15) Férey, G. *Chem. Soc. Rev.* **2008**, *37*, 191.

10.1021/ic8023265 CCC: $40.75
Published on Web 02/26/2009

phases MIL-53 (M(OH)BDC·guest),[16−18] MIL-68 (M(OH)-BDC·guest),[19,20] MIL-71 ($M_2(OH)_2F_2BDC$·guest),[21,22] MIL-88 (M_3OBDC_3·X·guest),[23] and MIL-101 (M_3OBDC_3·X·guest).[24] Among these, MIL-53 and MIL-88 (MIL = Materials of Institute Lavoisier) exhibit exceptional framework flexibility, and MIL-101 shows an unusually large pore volume and surface area. Due to its stability, the Al- and Fe-containing MIL-53 have been investigated intensively, for example in the fields of liquid−liquid separation,[8] gas sorption,[25,26] thin-film growth,[27] and drug delivery[28] and for Li-insertion reactions.[29] Recently, the amino-functionalized Fe form of MIL-53 ($Fe(OH)H_2N$−BDC·guest) has been described.[30]

In addition to the use of large linker molecules for the synthesis of isoreticular compounds containing larger pores, another main topic in MOF (metal−organic framework) chemistry is the functionalization of the pores. This is especially of interest for applications such as gas separation, gas storage, or host−guest chemistry, since it can lead to more selective materials or higher storage capacity. This can be achieved using reticular chemistry and employing functionalized organic molecules, such as derivatives of terephthalic acid.[31] For example, NH_2-, Br-, and CH_3-functionalized terephthalic acid has been employed in these investigations. An even more important aspect is the possibility to use these functional groups for postsynthetic modification reactions.[32] This has recently been demonstrated for the amino-functionalized MOFs, IRMOF-3[33−35] and IRMOF-16,[36] and a Gd-based framework[37] by acylation reaction with isonitriles, in some cases followed by metal complexation or bromination. ZIF-90 containing a carboxyaldehyde group has been modified by reduction with $NaBH_4$ and reaction with ethanolamine to yield an alcohol derivative and an imine functionality, respectively.[38] This synthetic strategy is expected to facilitate the generation of functional properties not directly accessible through conventional MOF synthesis. We have focused our research on the investigation of hybrid materials belonging to the MIL family, since these are thermally and chemically very stable compared to most other MOFs.

Table 1. Comparison of the Lattice Parameters of MIL-53,[16] and Fe−MIL-53−NH_2(as)[30] with the Results Obtained in This Work

sample	*a*/Å	*b*/Å	*c*/Å	*β*/°	*V*/Å^3
MIL-53(as)[16]	17.129(2)	6.628(1)	12.182(1)		1383.0(2)
MIL-53(lt)[16]	19.513(2)	7.612(1)	6.576(1)	104.24(1)	946.5(2)
MIL-53−NH_2(as)	16.898(20)	12.539(18)	6.647(8)	−	1408.4(4)
MIL-53−NH_2(DMF)	17.578(17)	11.483(9)	6.630(6)	−	1338.9(25)
MIL-53−NH_2(lt)	19.722(7)	7.692(3)	6.578(4)	105.1(3)	961.5(10)
MIL-53−NHCHO	17.156(5)	12.246(5)	6.604(13)		1387.4(8)
Fe−MIL-53−NH_2(as)[30]	17.668(3)	12.120(3)	6.9177(14)		1481.3(6)

Here, we report the synthesis of amino-functionalized, Al-containing MIL-53 and the activation by solvothermal and thermal treatment, as well as the postsynthetic modification using formic acid. For the detailed characterization of all the compounds powder XRD, IR, TG, and solid-state NMR measurements, as well as elemental analyses, were performed. In addition, results on N_2 sorption measurements are presented.

Experimental Section

Chemicals. $AlCl_3$·$6H_2O$ (Riedel−de Haen, ≥99%), NH_2−H_2BDC (Fluka, ≥98%), formic acid (Merck), and *N,N*-dimethylformamide (BASF, tech.) were used as obtained.

Methods. X-ray powder diffraction patterns were recorded with a STOE STADI P diffractometer equipped with a linear position-sensitive detector using monochromated Cu $K\alpha_1$ radiation. Lattice constants were determined using the DICVOL program[39] and refined using the STOE software package. Temperature-dependent X-ray diffraction experiments were performed in the Θ−Θ mode in air with the sample in the furnace (Anton Paar HTK 16 high-temperature chamber) of a Siemens D5000 diffractometer (Co radiation). Each powder pattern was recorded in the 8−25° range (2θ) at intervals of 10 °C up to 400 °C and 25 °C up to 500 °C with a 2 s/step scan, corresponding to an approximate duration of 1 h. The temperature ramp between two patterns was 10 °C min^{-1}. Thermogravimetric (TG) analyses were carried out in air or nitrogen (75 mL/min, 25−900 °C, 4 °C/min) on a Netzsch STA-409CD. Carbon, hydrogen, and nitrogen contents were determined by

(16) Loiseau, T.; Serre, C.; Huguenard, C.; Fink, G.; Taulelle, F.; Henry, M.; Bataille, T.; Férey, G. *Chem. Eur. J.* **2004**, *10*, 1373.
(17) Serre, C.; Millange, F.; Thouvenot, C.; Nogúes, M.; Marsolier, G.; Louër, D.; Férey, G. *J. Am. Chem. Soc.* **2002**, *124*, 13519.
(18) Millange, F.; Guillou, N.; Walton, R. I.; Grenèche, J.-M.; Margiolaki, I.; Férey, G. *Chem. Commun.* **2008**, 4732.
(19) Barthelet, K.; Marrot, J.; Ferey, G.; Riou, D. *Chem. Commun.* **2004**, 520.
(20) Volkringer, C.; Meddouri, M.; Loiseau, T.; Guillou, N.; Marrot, J.; Férey, G.; Haouas, M.; Taulelle, F.; Audebrand, N.; Latroche, M. *Inorg. Chem.* **2009**, in press.
(21) Barthelet, K.; Adil, K.; Millange, F.; Serre, C.; Riou, D.; Ferey, G. *J. Mater. Chem.* **2003**, *13*, 2208.
(22) Vougo-Zanda, M.; Anokhina, E. V.; Duhovic, S.; Liu, L.; Wang, X.; Oloba, O. A.; Albright, T.; Jacobson, A. J. *Inorg. Chem.* **2008**, *47*, 4746.
(23) Mellot-Draznieks, C.; Serre, C.; Surblé, S.; Audebrand, N.; Férey, G. *J. Am. Chem. Soc.* **2005**, *127*, 16273.
(24) Férey, G.; Mellot-Draznieks, C.; Serre, C.; Millange, F.; Dutour, J.; Surblé, S.; Margiolaki, I. *Science* **2005**, *309*, 2040.
(25) Bourrelly, S.; Llewellyn, P. L.; Serre, C.; Millange, F.; Loiseau, T.; Férey, G. *J. Am. Chem. Soc.* **2005**, *127*, 13519.
(26) Llewellyn, P. L.; Bourrelly, S.; Serre, C.; Filinchuk, Y.; Férey, G. *Angew. Chem.* **2006**, *118*, 7915.
(27) Scherb, C.; Schödel, A.; Bein, T. *Angew. Chem., Int. Ed.* **2008**, *120*, 5861.
(28) Horcajada, P.; Serre, C.; Guillaume, M.; Ramsahye, N. A.; Balas, F.; Vallet-Regí, M.; Sebban, M.; Taulelle, F.; Férey, G. *J. Am. Chem. Soc.* **2008**, *130*, 6774.
(29) Férey, G.; Millange, F.; Morcrette, M.; Serre, C.; Doublet, M.-L.; Grenèche, J.-M.; Tarascon, J.-M. *Angew. Chem., Int. Ed.* **2007**, *46*, 3259.
(30) Bauer, S.; Serre, C.; Devic, T.; Horcajada, P.; Marrot, J.; Férey, G.; Stock, N. *Inorg. Chem.* **2008**, *47*, 7568.
(31) Yaghi, O. M.; O'Keefe, M.; Ockwig, N. W.; Chae, H. K.; Eddaoudi, M.; Kim, J. *Nature* **2003**, *423*, 705.
(32) Wang, Z.; Cohen, S. M. *J. Am. Chem. Soc.* **2007**, *129*, 12368.
(33) Dugan, E.; Wang, Z.; Okamura, M.; Medina, A.; Cohen, S. M. *Chem. Commun.* **2008**, *29*, 3366.
(34) Wang, Z.; Cohen, S. M. *Angew. Chem., Int. Ed.* **2008**, *120*, 4777.
(35) Ingleson, M. J.; Barrio, J. P.; Guilbaud, J.-B.; Yaroslav, Z.; Khimyak, Y. Z.; Rosseinsky, M. J. *Chem. Commun.* **2008**, *23*, 2680.
(36) Goto, Y.; Sato, H.; Shinkai, S.; Sada, K. *J. Am. Chem. Soc.* **2008**, *130*, 14354.
(37) Costa, J. S.; Gamez, P.; Black, C.; Roubeau, O.; Teat, S. J.; Reedijk, J. *Eur. J. Inorg. Chem.* **2008**, 1551.
(38) Morris, W.; Doonan, C. J.; Furukawa, J. H.; Banerjee, R.; Yaghi, O. M. *J. Am. Chem. Soc.* **2008**, *130*, 12626.
(39) Boultif, A.; Louer, D. *J. Appl. Crystallogr.* **1991**, *24*, 987.

elemental chemical analysis on an Eurovektor EuroEA Elemental Analyzer. IR spectra were recorded on an ATI Matheson Genesis in the spectral range 4000−400 cm^{-1} using the KBr disk method. EDX analysis was performed on a Philips ESEM XL 30. ^{15}N, ^{13}C, ^{27}Al and ^{1}H solid-state NMR studies were performed on a commercial BRUKER Avance II 300 spectrometer operating at 7.05 T with resonance frequencies of 30.4, 75.5, 78.2 and 300.1 MHz, respectively. ^{1}H and ^{13}C shifts were referenced relative to TMS, ^{15}N shifts with respect to nitromethane, and ^{27}Al shifts relative to $AlCl_3$ in an acidic aqueous solution. Samples for ^{13}C and ^{15}N measurements were filled in standard 4 mm ZrO_2 rotors and mounted in a triple-resonance probe (Bruker). For all ^{13}C and ^{15}N experiments, spinning frequencies between 4.5 and 12 kHz were set. ^{1}H and ^{27}Al spectra were recorded with a triple resonance 2.5 mm MAS probehead and spinning frequencies of 25 kHz and 30 kHz, respectively. A ramped cross-polarization sequence with contact times between 3 and 5 ms was employed to excite ^{13}C and ^{15}N nuclei via the proton bath, where the power of the ^{1}H radiation was linearly varied from 100 to 50%. For the acquisition of the ^{1}H spectra, three back-to-back 90° pulses were used in order to eliminate unwanted contributions from the probe.[30] The 90° pulse length was adjusted to 3 μs, and the recycle delay varied between 2.5 and 10 s to guarantee total rebuild of magnetization due to spin−lattice relaxation. ^{27}Al spectra were recorded with a Hahn−Echo sequence with pulse lengths of 1.0 and 2.0 μs for the first and second impulses and a nutation frequency of 65 kHz. All 1D experiments were recorded using broadband proton decoupling via the SPINAL64 sequence.[29] The ^{27}Al MQ-MAS spectra were measured in standard 4 mm ZrO_2 rotors with a rotation frequency of 12.5 kHz, using a three-pulse sequence[40] with nutation frequencies of 100 and 13 kHz for the excitation, conversion, and selective 90° pulses, respectively. The coherence pathway 0 ± 30−1 was selected via a cog-wheel phase cycle[41] COG60{11,1,0;30}, and the repetition delay was set to 0.5 s.

The sorption behavior of the dehydrated MIL-53−NH_2(lt) (lt = activated, low temperature phase)[16,30] and MIL-53−NHCHO was determined measuring the N_2 sorption isotherms at 77 K using a Bellsorp Max apparatus. Based on the TG data, activation at 130 °C under vacuum for 3 h was used. Due to the presence of a strong hysteresis in the initial sorption measurements, the same sample was measured four times with a repeated activation at 130 °C for 3 h in between the measurements.

Synthesis. Al−MIL-53−NH_2(as), Al(OH)[H_2N−BDC]·0.3-(H_2N−H_2BDC). The discovery, as well as the optimization under solvothermal conditions, was done using our high-throughput methodology.[42−44] Thus, syntheses were performed in the range of 110−180 °C. The following aluminum salts were employed in the investigation: $Al(NO_3)_3 \cdot 9H_2O$, $Al(ClO_4)_3 \cdot 9H_2O$, and $AlCl_3 \cdot 6H_2O$. Different protic as well as aprotic solvents (acetonitrile, DMF, methanol, and water) were used. From more than 350 experiments, the following optimal reaction conditions were extracted: (1) H_2O is the best solvent; (2) the molar ratio Al^{3+}:H_2N−H_2BDC of 1:1 is the best; (3) the temperature should be around 150 °C since lower temperatures lead to less crystalline products, while at higher temperatures the decomposition of H_2N−H_2BDC is observed. The optimized synthesis parameters were employed for the scale-up reaction. This reaction was carried out in a 27 mL Teflon-lined steel bomb under autogenous pressure for 5 h at 150 °C. The molar ratio Al^{3+}:H_2N−H_2BDC:H_2O of 1:1:153 was used ($AlCl_3 \cdot 6H_2O$ (493.6 mg), H_2BDC−NH_2 (375.6 mg), and 5 mL H_2O). After filtering and washing with deionized water, the resulting yellow product (yield: 50% based on H_2BDC−NH_2) was first identified by X-ray powder diffraction analysis (Table 1). The amount of included H_2N−H_2BDF was determined by TG analysis.

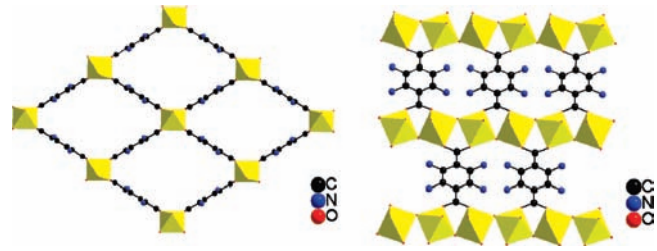

Figure 1. View along (left) and perpendicular to (right) the pore system in MIL-53−NH_2 (disordered H_2N−H_2BDC molecules in the pores have been omitted for clarity). The MO_6-octahedra are presented in yellow. N positions are only occupied by one-fourth.

Activation of MIL-53−NH_2(as), Al(OH)[H_2N−BDC]·0.3-(H_2N−H_2BDC). The as form contains free aminoterephthalic acid, which could not be removed by thermal activation. This could be due to stronger host−guest interactions owing to the NH_2 groups. A two-step procedure led to the activated form. In the first step, aminoterephthalic acid in pores was exchanged by DMF at 150 °C. Thus, MIL-53−NH_2(DMF), Al(OH)[H_2N−BDC]·0.95DMF, was formed (calcd C: 44.5, H: 4.4, N: 9.3; obsd C: 44.7, H: 4.4, N: 9.3). The DMF molecules were removed by thermal treatment in air at 130 °C in a muffle furnace. Upon cooling in air, MIL-53−NH_2(lt), Al(OH)[H_2N−DC]·0.9H_2O, was obtained (calcd C: 40.1, H: 3.3, N: 5.8; obsd: C: 40.1, H: 3.2, N: 5.7). For the postsynthetic modification, the lt-form was used.

Postsynthetic Modification of MIL-53−H_2(lt). To 200 mg of Al(OH)[H_2N−DC]·0.9H_2O (0.8 mmol), 200 μL of formic acid (5.3 mmol) was added in a glass flask. The reaction at 70 °C for 3 h, followed by washing with H_2O and heating in air (130 °C, 2 days), leads to the formation of formamide groups (Al−MIL-53−NHCHO, Al(OH)[OHCN−BDC]·H_2O) (elemental analysis, calcd: C: 40.2, H: 3.0, N: 5.2; obsd: C: 40.2, H: 3.2, N: 5.2).

Results and Discussion

The synthesis of amino-functionalized Al−MIL-53 was accomplished. The activation of the pores was carried out by solvent exchange and thermal treatment. The activation of the water-containing form at elevated temperatures leads to a porous compound, and the postsynthetic modification using formic acid as a reactant is possible (Scheme 1).

Structure Description. The framework topology of all title compounds is identical, and they correspond to the MIL-53 structure (Figure 1). This structure contains chains of μ-OH corner-sharing AlO_6-octahedra, which are interconnected by aminoterephthalic acid molecules to form one-dimensional pores. Based on results of the lattice constant determinations, the structures of the different forms of MIL-53−NH_2 were found to correspond to the ones observed in the nonfunctionalized system (Al−MIL-53) and the other known amino-functionalized compound, Fe−MIL-53−NH_2(as) (Table 1). Similar breathing behavior of the frameworks is observed, which is due to host−guest interactions.

(40) Amoureux, J. P.; Fernandez, C.; Steuernagel, S. *J. Magn. Reson. A* **1996**, *123*, 116.
(41) Jerschow, A.; Kumar, R. *J. Magn. Reson.* **2003**, *160*, 59.
(42) Bauer, S.; Stock, N. *Angew. Chem., Int. Ed.* **2007**, *46*, 6857.
(43) Bauer, S.; Bein, T.; Stock, N. *Inorg. Chem.* **2005**, *44*, 5882.
(44) Stock, N.; Bein, T. *Angew. Chem., Int. Ed.* **2004**, *43*, 749.

Scheme 1. Postsynthetic Modification of MIL-53−NH_2 by Reaction with Formic Acid

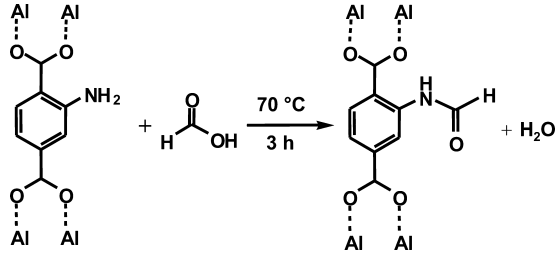

As observed for the Fe-containing compound, the as-synthesized MIL-53−NH_2(as), Al(OH)[H_2N−BDC]·0.3-(H_2N−H_2BDC), contains free aminoterephthalic acid molecules in the pores, and the NH_2 group is disordered over four crystallographically equivalent positions. The free aminoterephthalic acid molecules can be exchanged by treatment with DMF, and MIL-53−NH_2(DMF), Al(OH)-[H_2N−BDC]·0.95DMF, is formed. This guest exchange leads only to minor changes in the cell parameters. After thermal removal of the DMF molecules, followed by cooling to RT under ambient conditions, a drastic change in cell symmetry from orthorhombic to monoclinic and in cell parameters is observed. The same results are found for MIL-53, and the contraction of the rhombic channels is due to the formation of strong hydrogen bonds between the water molecules and the carboxylate groups of the framework. Thus, the presence of NH_2 seems to have only minor influence on the structure. Upon postsynthetic modification, the unit cell symmetry changes back from monoclinic to orthorhombic symmetry, and cell parameters are similar to the ones found for MIL-53−NH_2(as) and MIL-53−NH_2(DMF).

Thermal Behavior. The thermal behavior of the four compounds was studied by TG measurements (Figure 2). In addition, an X-ray thermodiffractogram of MIL-53−NH_2(as) in air (Figure 3) is presented. All TG curves show a two-step weight loss. The first step corresponds to the release of the guest molecules within the pores, and the second weight loss is due to the decomposition of the aminoterephthalic acid from the framework. The first steps in these diagrams, as well as the CNHS analyses, were used to calculate the amount of different guest molecules.

In contrast to MIL-53(as) and Cr−MIL-53(as), the free acid molecules depart at lower temperatures (220 vs 275 °C). The observed weight loss of 20% (0.30 mol of H_2BDC per formula unit) is smaller than the one observed in the pure terephthalic acid compounds, but it is in accordance with results from Fe−MIL53(as). The departure is accompanied by a structural change and followed by the decomposition of the structure. This is clearly observed in the X-ray thermodiffractogram (Figure 3), where two structural changes occur upon heating. Up to 250 °C, almost no changes of the reflex intensities and positions of MIL-53−NH_2(as) are detectable. This temperature is slightly higher than the one from the TG study. Around 250 °C, a drastic shift of the reflection positions is found, which is accompanied by peak broadening. Above 410 °C, no crystalline products are observed. MIL-53−NH_2(as) is transformed into an X-ray amorphous product.

The solvent-exchanged sample MIL-53−NH_2(DMF), Al(OH)[H_2N−BDC]·0.95DMF, releases the DMF molecules upon heating up to 320 °C (Figure 2 top right). The observed weight loss (23%) corresponds to 0.95 equiv of DMF molecules, which is also confirmed by elemental analysis. The solvent-free structure is stable up to approximately 400 °C, and it collapses at higher temperatures.

The water-containing samples, MIL-53−NH_2(lt), Al(OH)-[H_2N−BDC]·0.9H_2O, and MIL-53−NHCHO, Al(OH)-[HC(O)N(H)−BDC]·H_2O, show very similar TG curves. The dehydration of both compounds is observed up to 150 °C. The weight loss corresponds to 0.9 and 1 mol equivalent water molecules per formula unit for MIL-53−NH_2(lt) and MIL-53−NHCHO, respectively. The framework structures are stable up to 400 °C. Thus, the exceptional thermal stability of the nonfunctionalized MIL-53(lt), where a decomposition temperature of 500 °C is observed, is not found.

Sorption Experiments. MIL-53−NH_2(lt) was activated at 130 °C in vacuum for 3 h. In contrast to MIL-53, the sorption curves of MIL-53−NH_2 (Figure 4) show hysteresis behavior, which strongly depends on the number of sorption/desorption cycles and activation steps. While in the first two measurements sorption occurs at higher partial pressures, reproducible results are obtained starting with the third measurement. This could be due to the presence of guest molecules that are only removed after repeated measurements and activation.

Infrared Spectroscopy. The IR spectra of MIL-53−NH_2-(as), MIL-53−NH_2(DMF), and Al−MIL-53−NH_2(lt) are shown in Figure 5. The activation steps can clearly be followed. The spectrum of MIL-53−NH_2(as) exhibits the typical vibrational bands in the region of 1400−1700 cm^{-1} for the carboxylic acid function of the Al-coordinating and free aminoterephthalic acid.[16,30] The different O−H and N−H groups can be clearly seen. The bands at 3656 and 3497/3385 cm^{-1} and the broad signals between 3000 and 2500 cm^{-1} are due to the bridging OH and the NH_2 group, as well as the aminoterephthalic acid in the pores, respectively. The latter bands are absent in the spectrum of MIL-53−NH_2(DMF), and additional bands due to the presence of CH_3 groups are observed. The C═O band of the free acid (1687 cm^{-1}) in the pores is replaced by the C═O band of the DMF molecules (1670 cm^{-1}). These bands vanish upon thermal treatment under formation of Al−MIL-53NH_2(lt).

The postsynthetic modification under formation of the formamide functionality (Figure 6) is clearly demonstrated by the appearance of bands that are due to the formation of an amide.[45] The two sharp bands of the NH_2 group vanish and one broad band is observed. New signals at 1690, 1296 cm^{-1} are caused by the C═O and the C−N stretching vibration of the formamide. At the same time, the bands due to the C−N(NH_2) vibration at 1254 and 1334 cm^{-1} appear with much lower intensities. This indicates a partial functionalization of the NH_2 groups.

(45) Socrates, G. *Infrared and Raman Characteristic Group Frequencies: Tables and Charts*, 3rd ed.; Wiley & Sons: West Sussex, U.K., 2004.

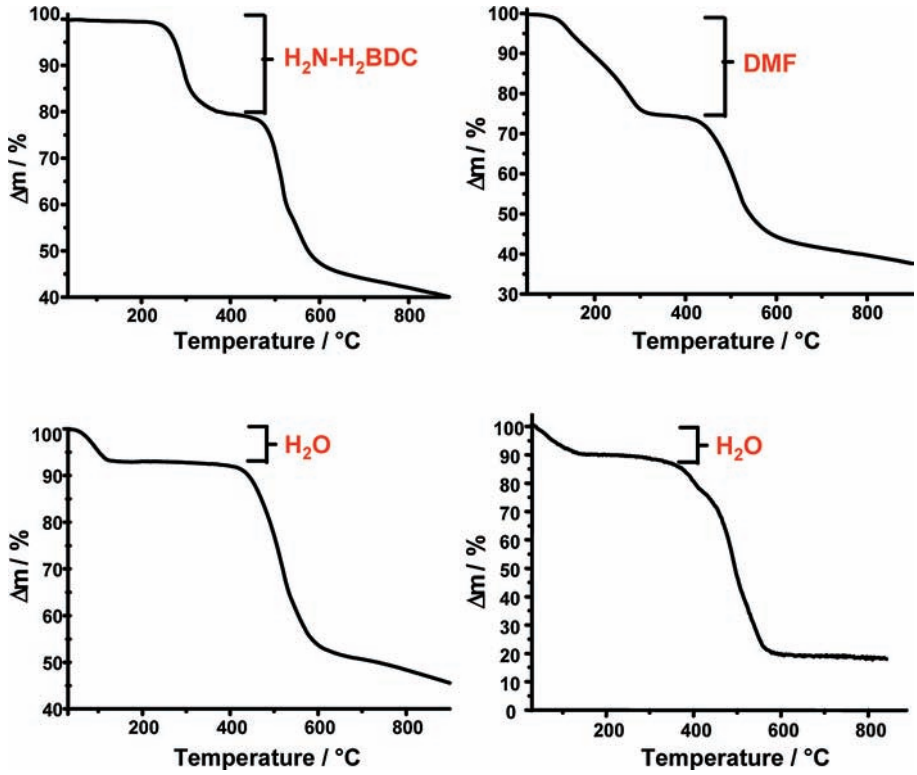

Figure 2. TG curves of MIL-53−NH_2(as), MIL-53−NH_2(DMF), MIL-53−NH_2(lt) under nitrogen, and TG curves of MIL-53-NHCHO under oxygen.

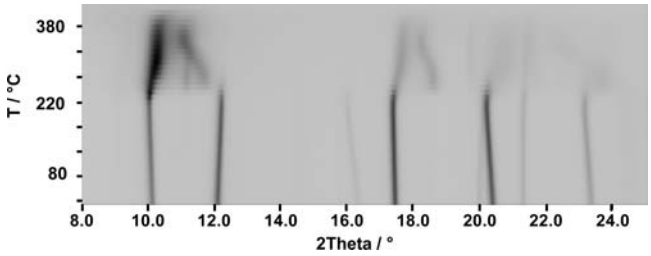

Figure 3. Results of the temperature-dependent X-ray powder XRD study of MIL-53−NH_2(as) in air (20−500 °C).

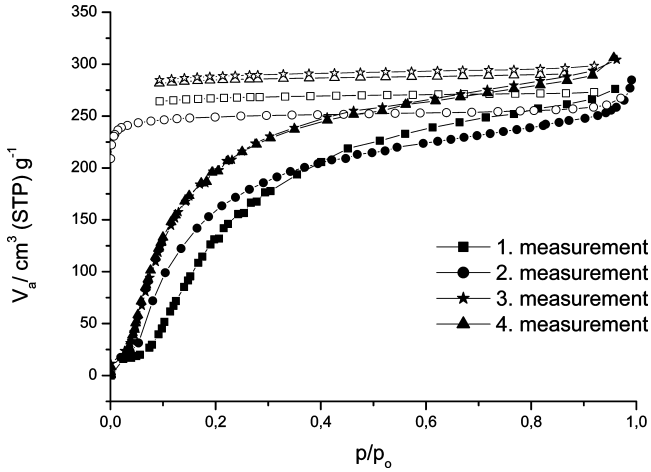

Figure 4. N_2 sorption isotherms of MIL-53−NH_2(lt) activated for 3 h at 130 °C before each measurement. The same sample was measured four times, applying the same activation procedure prior to the measurements. Black symbol denotes sorption and white symbol denotes desorption curves.

Solid-State NMR Studies. The ^{1}H, ^{13}C, ^{15}N, and ^{27}Al MAS NMR spectra of MIL-53−NH_2(as,DMF,lt) and MIL-53−NHCHO are displayed in Figures 7−10. The assignment of the bands is based on literature data.[16,46,47] The NMR spectra show signals due to the different guest species in the pores. Figure 7 displays the ^{1}H spectra of the four compounds. The as form exhibits three signals at $\delta = 2.3$, 6.4, and 12.2 ppm due to the μOH bridging hydroxide groups, the aromatic CH atoms, and the COOH groups, respectively. The ^{1}H spectrum of the DMF form shows peaks at $\delta = 1.5$, 2.3, and 7.3 ppm attributable to the CH_3 groups of the DMF, the μOH bridging hydroxide groups, and the aromatic CH atoms. No signals due to the free aminoterephthalic acid are observed. The spectrum of MIL-53−NH_2(lt) shows three signals at $\delta = 2.6$, 4.5, and 6.4 ppm that can be assigned to the μOH, H_2O, and aromatic CH atoms, respectively. In accordance with MIL-53(lt), the last two signals are poorly resolved and broad.[16] It should be noted that the ^{1}H resonances arising from the amino groups for MIL-53−NH_2(as,DMF,lt) are expected between 6 and 8 ppm and are, thus, obscured by the proton signals in the aromatic region. The ^{1}H spectrum of MIL-53−NHCHO exhibits one broad signal at 10.9 ppm that can be assigned to the formamide group. Its low-field shift may be caused by hydrogen bond interactions with two water molecules in the cages. In addition, the signals of the phenyl ring and the μOH bridging hydroxide groups at 7.4 and 2.7 ppm, respectively, are observed.

The ^{13}C and ^{15}N NMR spectra clearly demonstrate the postsynthetic modification under formation of the formamide group. The ^{13}C NMR spectrum of MIL-53−NH_2(as) (Figure 8a) exhibits five broad signals, four between $\delta = 149.6$ and

(46) Jürgens, B.; Irran, E.; Senker, J.; Kroll, P.; Müller, H.; Schnick, W. *J. Am. Chem. Soc.* **2003**, *125*, 10288.
(47) Smernik, R. J.; Baldock, J. A. *Plant Soil* **2005**, *275*, 271.

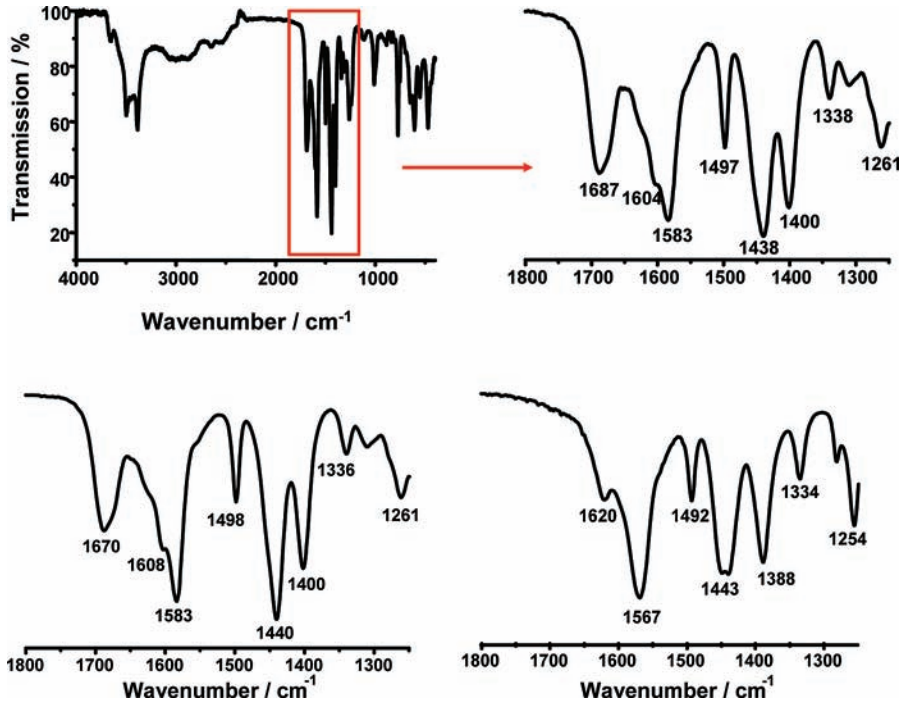

Figure 5. Top: IR spectrum of MIL-53−NH_2(as). Bottom: MIL-53−NH_2(DMF) (left) and MIL-53−NH_2(lt) (right).

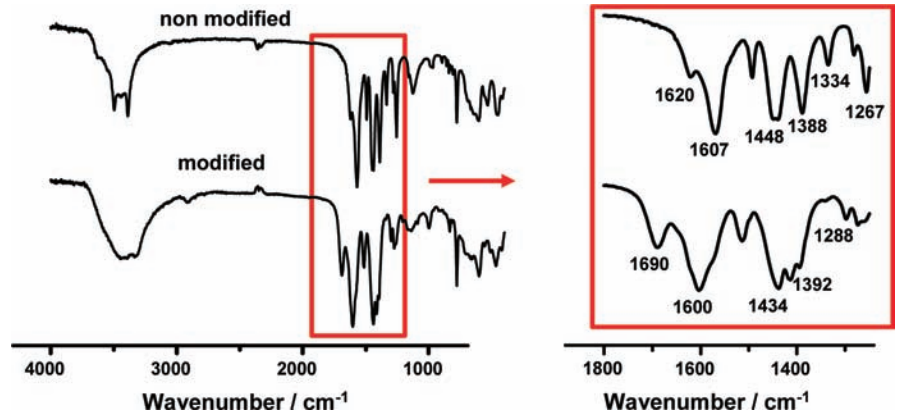

Figure 6. IR spectra of MIL-53−NH_2(lt) (top) and modified MIL-53−NHCHO (bottom).

117 ppm, due to the C atoms of the phenyl ring and one signal at $\delta = 172$ ppm, which is caused by the carboxylic groups. The ^{13}C spectrum of the DMF form shows three additional signals at $\delta = 29.1$, 35.2, and 163.4 ppm attributable to the DMF molecules. In the ^{13}C spectrum of the lt form, these signals are not present. The peak of the carboxylate group is shifted in the lt form from $\delta = 172.4$ to 176.7 ppm due to the presence of water molecules and the change in the crystallographic symmetry.[16] The signals of the phenyl rings are much better resolved. Upon postsynthetic modification, a new signal at 160.8 ppm is observed, which is caused by the presence of the formamide functionality. The other signals show only minor changes.

The ^{15}N NMR spectra of the as, DMF and lt form exhibit a signal in the region from $\delta = -312$ to -315 ppm, which can be unequivocally assigned to the NH_2 group. An additional sharp intensive signal in the spectrum of the DMF form is observed at $\delta = -274.2$ ppm and is attributed to the DMF molecules in the pores. The ^{15}N MAS NMR spectrum of MIL-53−NHCHO exhibits two signals at -315.2 and -248.8 ppm. The former is due to the presence of unreacted NH_2 groups, while the latter gives evidence to the successful postsynthetic modification under formation of the formamide.[46] Considering the cross-polarization time of 3 ms, which overemphasizes the NH_2 group, the functionalization can be regarded as almost complete.

The 1D ^{27}Al NMR spectra are shown in Figure 10. All spectra can be interpreted in accordance with a single resonance with an isotropic shift around 0 ppm, and a shape which is dominated by a second order quadrupole interaction. As for MIL-53, this is consistent with only one type of AlO_6 octahedra present in the crystal structure for all compounds.[16] Due to the local disorder caused by the functionalization of the terephthalic acid molecules, the ^{27}Al MAS spectra acquired for MIL-53−NH_2(as,DMF,lt) and MIL53−NHCHO are much more featureless than for the pure MIL-53.[16] The distribution of chemical shift values and quadrupolar coupling constants is also reflected in the TQ dimension of MQMAS spectra (shown only for MIL-53−NHCHO in Figure 11). The lack of other aluminum species especially

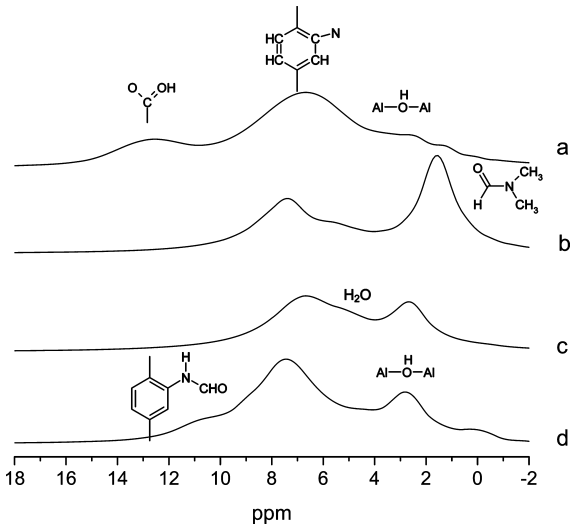

Figure 7. ^{1}H MAS NMR spectra of (a) MIL-53−NH_2(as), (b) MIL-53−NH_2(DMF), (c) MIL-53−NH_2(lt) and (d) MIL-53−NHCHO.

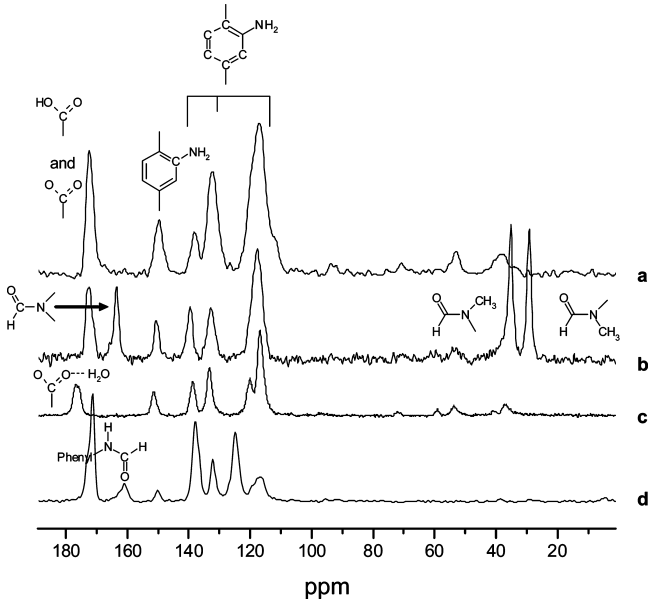

Figure 8. ^{13}C MAS NMR spectra of (a) MIL-53−NH_2(as), (b) MIL-53−NH_2(DMF), (c) MIL-53−NH_2(lt) and (d) MIL-53−NHCHO.

in the MQMAS spectrum of MIL-53−NHCHO, however, indicates that the postsynthetic functionalization can be carried out without formation of side products. The trends for the line width of the ^{27}Al spectra, which increases from MIL-53−NH_2(as) (QCC = 2.3 MHz) over MIL-53−NHCHO (QCC = 2.4 MHz) and MIL-53−NH_2(DMF) (QCC = 2.5 MHz) over MIL-53−NH_2(lt) (QCC = 2.7 MHz), are correlated with an increasing distortion of the channels in the MIL-53 structure, leading to a more anisotropic environment of the AlO_6 octahedra. Thus, the overall line width can be used as a simple probe for the space requirement of the incorporated guest molecules.

Conclusion

The chemically and thermally very stable MOF MIL-53-containing NH_2 groups, i.e. MIL-53−NH_2, has been obtained and used in the postsynthetic modification by reaction with

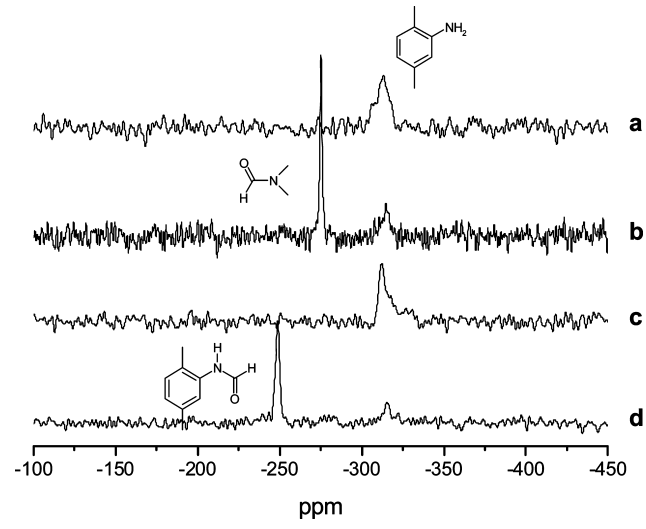

Figure 9. ^{15}N MAS NMR spectra of (a) MIL-53−NH_2(as), (b) MIL-53−NH_2(DMF), (c) MIL-53−NH_2(lt) and (d) MIL-53−NHCHO.

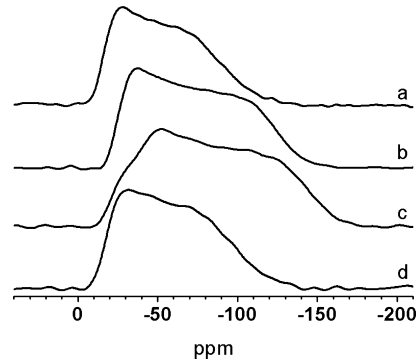

Figure 10. ^{27}Al MAS NMR spectra of (a) MIL-53−NH_2(as), (b) MIL-53−NH_2(DMF), (c) MIL-53−NH_2(lt) and (d) MIL-53−NHCHO.

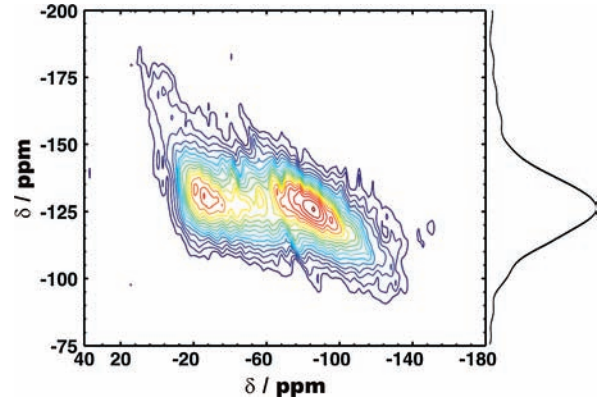

Figure 11. ^{27}Al MQMAS NMR spectrum of MIL-53−NHCHO.

formic acid. The activation of the as synthesized compound containing free aminoterephthalic acid molecules is accomplished in a two-step process. Thus, three forms of MIL-53−NH_2 have been obtained and thoroughly characterized. In comparison to MIL-53, the thermal stability of the amino-functionalized MIL-53−NH_2 is decreased. As shown by powder XRD measurements, the presence of the NH_2 group has no obvious influence on the breathing behavior of the aluminum carboxylate framework. This is only influenced by the presence of hydrogen bonds between the water molecules and the carboxylate groups. A strong difference

is observed in the N_2 sorption behavior. Strong hysteresis is found in the amino-functionalized compound. The postsynthetic modification of the activated MIL-53−NH_2 was accomplished by reaction with formic acid and verified by a combination of NMR and IR analysis.

Acknowledgment. The work has been supported by the German Science Foundation (DFG) via the DFG priority program SPP 1362 Porous Metal-Organic Frameworks under grants STO 643/5-1 and SE 1417/4-1.

Supporting Information Available: Powder XRD pattern results for (a) MIL-53−NH_2(as), (b) MIL-53−NH_2(DMF), (c) MIL-53−NH_2(lt) and (d) MIL-53−NHCHO. This material is available free of charge via the Internet at http://pubs.acs.org.

IC8023265